Morphology and magnetic properties of thin films of Rh on highly oriented pyrolitic graphite

A. Goldoni,[1] A. Baraldi,[1] G. Comelli,[2,3] F. Esch,[2] R. Larciprete,[1,4] S. Lizzit,[1] and G. Paolucci[1]
[1]*Sincrotrone Trieste SCpA, s.s. 14 Km 163.5 in Area Science Park, 34012 Trieste, Italy*
[2]*Laboratorio TASC-INFM, s.s. 14 Km 163.5 in Area Science Park, 34012 Trieste, Italy*
[3]*Dipartimento di Fisica, Università di Trieste, Via Valerio 2, 34127 Trieste, Italy*
[4]*ENEA, Divisione di Fisica Applicata, Via E. Fermi 45, 00044 Frascati (RM), Italy*
(Received 6 June 2000; revised manuscript received 5 October 2000; published 29 December 2000)

The structure and magnetic properties of ultrathin Rh layers deposited on highly oriented pyrolitic graphite (HOPG) have been investigated by means of core-level photoemission and scanning tunneling microscopy. The Rh growth on HOPG follows the Volmer-Weber mode at 300 K for any coverage, while Rh may form a commensurate $p(1\times1)$ ordered structure when deposited at 150 K for a coverage up to one monolayer. For submonolayer or monolayer Rh films on HOPG the linear magnetic dichroism in the angle distribution of photoelectrons shows no evidence of in-plane long-range magnetic ordering.

DOI: 10.1103/PhysRevB.63.0354XX PACS number(s): 79.60.Dp, 75.70.Ak, 68.35.Bs, 68.55.Jk

I. INTRODUCTION

The growth of thin films, atomic chains, and clusters of transition metals on single-crystalline surfaces is of considerable interest for researchers, because it represents an unprecedented scientific and technological opportunity for designing interesting magnetic materials and devices. All these objects have the common characteristic that the length scales are small enough to exhibit quantum phenomena and, therefore, unusual electronic and/or magnetic properties can be expected.[1–3] In the last decade, theory and experiments have opened the door to a whole class of low-dimensional systems, where the combination of large spin-orbit interaction and large local magnetic moments can produce sizable magnetocrystalline anisotropy with interesting effects on electronic, thermodynamic and magneto-optical behaviors.[1–7]

In the search for ultrathin magnetic systems one is not restricted to those transition metals that exhibit magnetism in the bulk. Recent experimental and theoretical efforts have addressed the question of a possible onset of ferro- or antiferromagnetism in nanostructures, free-standing clusters, thin films, and surfaces of metals that are nonmagnetic in the bulk form. Sc, Ti, V, Pd, Rh, and Ru have been singled out as potential candidates, Rh and Ru being the most promising ones.[1,8–28] Since these metals almost satisfy the Stoner criterion of ferromagnetism in the bulk, they can become magnetic if the density of states at the Fermi level is enhanced due to either an expansion of the lattice parameter or a reduced atomic coordination number.

Calculations predict that Rh could be magnetic in the form of a single layer on Ag(001) and Au(001),[14–16] or as free-standing clusters of less than a hundred atoms,[11–13] while it is at the onset of ferromagnetism at the Rh(100) surface.[29] Experimentally, indeed, magnetic ordering has been found for the Rh(100) surface[30] and for Rh clusters.[31] However, a Rh monolayer on Ag or Au was found experimentally nonmagnetic.[23,26] The reason for this could be related to the experimental difficulties of growing these $4d$ elements as ordered monolayers on Ag and Au. The growth process depends dramatically on the experimental conditions, such as the substrate temperature and cleanliness, the deposition rate, etc. In addition, most transition metal monolayer systems on noble metal substrates are not in thermodynamic equilibrium and diffusion of transition metal adatoms into the substrate represents a serious problem.[1]

To overcome some of these experimental problems, graphite has been suggested as an alternative substrate since transition metal atoms diffuse much less into it.[20,21,24,28,32–35] The graphite (0001) surface is furthermore known to be very flat and, as in the case of noble metals, the overlap with the transition metal d band is expected to be small.[28,32–35] Moreover, spin-polarized secondary-electron emission spectroscopy[24] applied to 1 ML (monolayer) of Ru on highly oriented pyrolitic graphite (HOPG) seems to confirm the presence of bidimensional ferromagnetism in this system. This evidence of magnetism in a $4d$ monolayer is very encouraging and prompts verification with other experimental techniques and other $4d$ materials like Rh.

In this paper we study the growth of Rh thin layers on HOPG at 150 K and room temperature (300 K) using x-ray photoemission spectroscopy (XPS) and scanning tunneling microscopy (STM). By exploiting the element specificity and surface sensitivity of photoemission, the presence of in-plane magnetic order in these systems has been investigated by looking for linear magnetic dichroism in angular distribution (LMDAD) effects in the core-level photoemission experiments. We show that Rh monolayers and/or submonolayers on HOPG(0001) do not present in-plane magnetic order down to 150 K and that this is probably due to the interaction with the substrate.

II. EXPERIMENT

The angle-resolved core-level photoemission measurements were performed in the ultra-high vacuum experimental chamber (base pressure 8×10^{-11} mbar) of the SuperESCA beamline at ELETTRA in Trieste,[36] using linearly polarized light. The photoelectrons were collected by means of a 150 mm hemispherical electron energy analyzer, with an overall energy resolution better than 60 meV and an angular resolution of $\pm2°$. Scanning tunneling microscopy was performed in a different UHV experimental chamber (base pressure 8

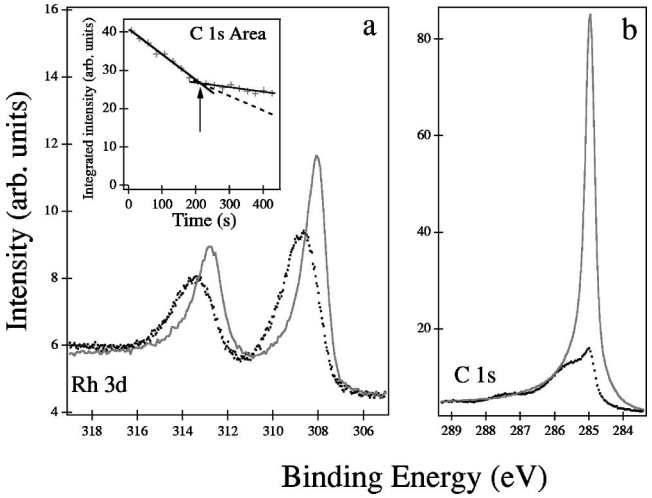

FIG. 1. (a) Rh 3*d* core-level photoemission spectra of a Rh film about 2 ML thick, as deposited at 150 K (dots) and after annealing at 300 K (line). Inset: Integrated intensity of the C 1*s* core-level photoemission spectrum as a function of time during the Rh deposition at 150 K. The arrow indicates the breakpoint corresponding to the completion of the first Rh layer. The dashed line is the expected behavior in the case of a layer-by-layer growth. (b) C 1*s* core-level photoemission spectra of the HOPG substrate just after the deposition of about 2 ML of Rh at 150 K (dots) and after annealing at 300 K (line).

$\times 10^{-11}$ mbar) using the standard Omicron VT STM at room temperature. This chamber was also equipped with a low-energy electron diffraction (LEED)/Auger apparatus.

The HOPG substrate was cleaved in air and immediately inserted in the experimental chambers via a fast entry lock. Repeated annealing cycles up to 1200 K were performed until a very sharp C1*s* core level was observed by XPS and no trace of contaminants was detected by photoemission and Auger electron spectroscopy (AES). Low background and very sharp spots, forming the typical rings, characterized the LEED pattern of the clean HOPG. For magnetic measurements, the sample was inserted in the gap of a horseshoe yoke electromagnet. The magnetic field was applied parallel to the sample surface and perpendicular to the photoemission scattering plane (chiral geometry[37]), by means of a current ramp through the electromagnet coil.

Rh deposition on the clean HOPG was performed in both UHV experimental chambers *in situ* using a homemade evaporator. The coverage was calibrated using AES and XPS.

III. RESULTS AND DISCUSSION

A. Growth and morphology of Rh films on HOPG

First we deposited Rh on the HOPG substrate kept at 150 K. We followed the Rh deposition in real time by collecting subsequent Rh 3*d* and C 1*s* core-level photoemission spectra at a photon energy of 400 eV. During the deposition the photoemission area of the C 1*s* core level decreased linearly as a function of time with a clear change in slope after 210 s [see inset of Fig. 1(a)]. This is consistent with either a layer-by-layer or a Stransky-Krastanov growth mode, and we assume that the change in slope indicates the completion of the first layer. To clarify this point, we have calculated the expected attenuation of the C 1*s* signal in the case of a layer-by-layer growth mode. Assuming an escape depth of 5 Å for photoelectrons of 120 eV kinetic energy, from the attenuation of the C 1*s* signal up to 1 ML we obtain a thickness of 2 Å for a single Rh layer. Using these parameters we can calculate the expected behavior (dashed line in the inset of Fig. 1) during the growth of the second Rh layer. There is a considerable disagreement between the calculations and the experimental attenuation of the C 1*s* signal. The C 1*s* is less attenuated than expected assuming a layer-by-layer growth, favoring therefore a Stransky-Krastanov growth mode at 150 K.

In Fig. 1 we report the high-resolution C 1*s* and Rh 3*d* core-level photoemission spectra just after the deposition of about 2 ML of Rh at 150 K (dots). The width and shape of both peaks are due to contributions from many components, which suggests the presence of several inequivalent atomic sites. The LEED pattern resembles that of the clean HOPG substrate, but with six spots, forming a hexagon, more intense than the others. This indicates that the first layer may form a commensurate $p(1\times1)$ structure of the Rh adatoms.

By raising the substrate temperature to 300 K, both Rh 3*d* and C 1*s* core levels become single sharp peaks, as also shown in Fig. 1 (solid line). The absolute spectral intensity of the C 1*s* core level strongly increases, suggesting that large graphite areas are now uncovered. This indicates a high mobility of the Rh adatoms at 300 K and, possibly, the formation of three-dimensional Rh islands. This behavior is in agreement with the substantial difference in surface energy between HOPG and Rh,[1] which favors the Volmer-Weber growth mode. The LEED pattern is the same of the clean HOPG. Annealing for 5 min to 450 K does not lead to further changes to the photoemission spectra and LEED pattern, indicating that some form of thermodynamic equilibrium has been achieved.

To further investigate the growth mode, we have also deposited an amount of Rh corresponding to about 3 ML (i.e., an evaporation time of ~650 s) on the clean HOPG substrate kept at 300 K. Figure 2 shows the evolution of the C 1*s* and Rh 3*d* peak areas in XPS during deposition. Both peaks follow a continuous, apparently exponential, behavior without any clear break point. The shape and the spectral intensity of these core levels are similar to those of the spectra measured after the annealing at 300 K of the Rh film deposited at 150 K (see Fig. 1). This behavior is consistent with the growth of three-dimensional (3D) islands at 300 K with large HOPG areas always uncovered during the growth (Volmer-Weber growth mode). In particular, as we will show in the Appendix, the unusual concave behavior of the increasing Rh 3*d* signal is consistent with the Volmer-Weber growth mode and indicates that in the early stages of growth the increase of the island volume dominates over an increase of the island number.

The morphology of about 2.2 ± 0.2 ML (based on Auger spectroscopy) of Rh deposited at 300 K has been investigated also with scanning tunneling microscopy. Figure 3

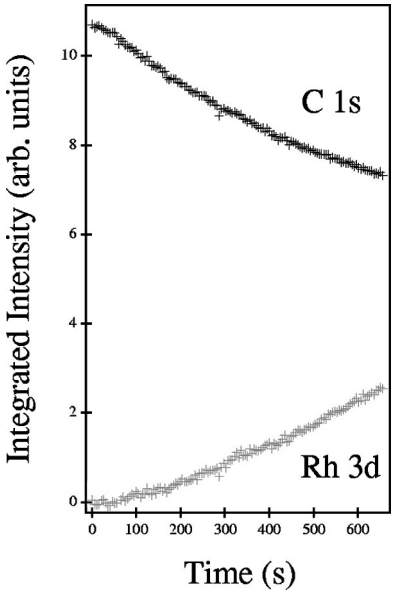

FIG. 2. Integrated intensity of the C 1*s* and Rh 3*d* core-level photoemission spectra as a function of time during Rh deposition at 300 K. The C 1*s* signal has been divided by a factor of 4 in order to plot the two curves on the same scale and enhance the exponential behavior.

shows a $2000\times2000\,\text{Å}^2$ STM image of this film, where a uniform distribution of Rh islands is visible on the HOPG substrate. The typical lateral size of these islands is about $100\times100\,\text{Å}^2$. These islands seem to have the tendency to agglomerate in groups of less than seven islands. The top panel of Fig. 4 reports a $200\times200\,\text{Å}^2$ STM image of a group of three islands showing that on top of the islands there is no clear atomic resolution. The inset highlights the atomic resolution on the HOPG substrate. The bright spots in the HOPG substrate image correspond to the β sites of the honeycomb graphite lattice, i.e., carbon atoms of the first layer just on top of the center of the hexagons of the second layer. The rough morphology of the Rh islands is clear from the height distribution (along the line cut shown on the top panel) reported in the bottom panel, which also indicates that these islands are formed by more than three Rh layers. The apparent vertical distance between the layers is about 2.8 Å, which must be compared with the step height expected for the low-index Rh surfaces, i.e., 2.2 Å for the (111), 1.9 Å for the (100), and 1.34 Å for the (110).

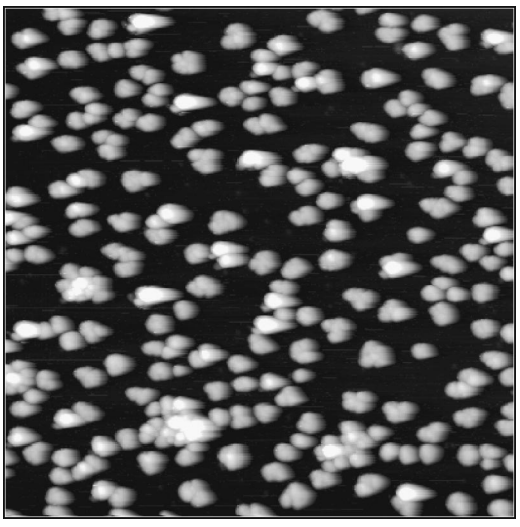

FIG. 3. $2000\times2000\,\text{Å}^2$ STM image of a Rh film deposited at 300 K, showing a quite uniform distribution of Rh islands on the HOPG substrate.

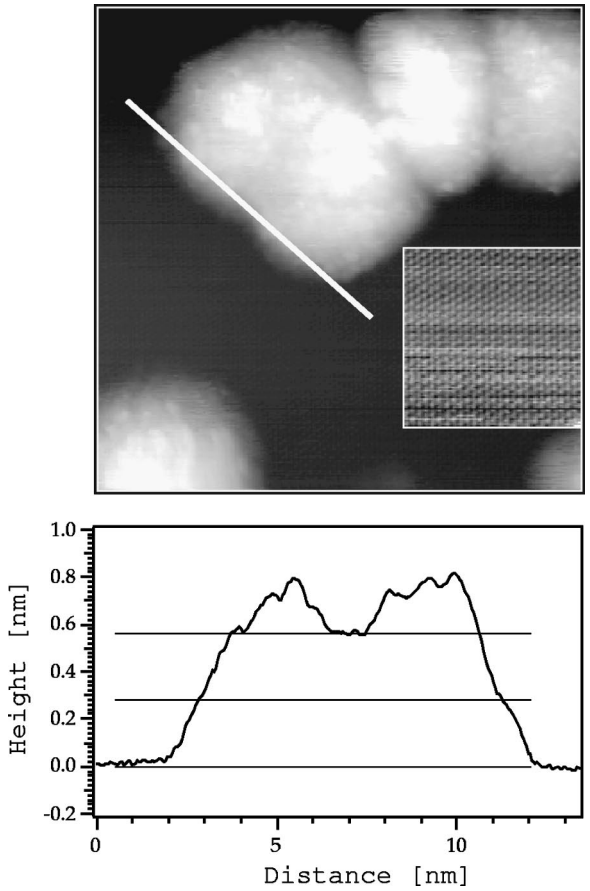

FIG. 4. Top: $200\times200\,\text{Å}^2$ STM image of a group of three Rh islands. The inset highlights the atomic resolution on the HOPG substrate. Bottom: Height distribution of a Rh island along the white line cut shown on the top panel. The horizontal lines indicate the positions of different planes.

Very rarely we can observe an isolated adatom. Figure 5 shows a $50\times20\,\text{Å}^2$ STM topography of an isolated adatom in a region of clean HOPG. The adatom is visible as enhancement of the site brightness that extends for about 5 Å around the β-site position occupied by the adatom (see also the bottom panel). The local enhancement of the corrugation is due to the high density of states at the Fermi level of the adatom, as compared to the *sp* states of the HOPG substrate, whose wave function extends away from the atomic position. The bottom panel of Fig. 5 indicates that the apparent height of the adatom is 1.0 Å, that is about five times the corrugation we measure on the clean HOPG substrate, but is much less than the height of one Rh layer in the 3D islands (2.8 Å). Moreover, the fact that this single adatom can be reproducibly imaged for several STM scans demonstrates that it is

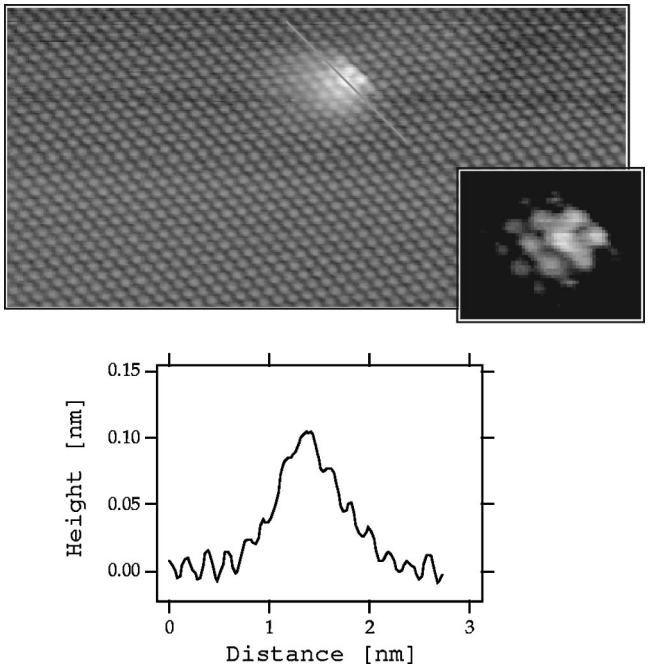

FIG. 5. Top: 50×20 Å^2 STM topography of an isolated metallic adatom on a β site of clean HOPG. The inset highlights the site brightness enhancement around the metallic adatom. Bottom: Apparent height distribution along the line cut shown on the top panel.

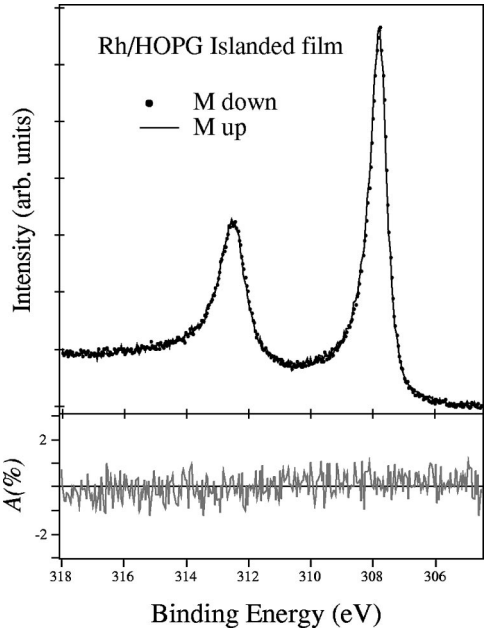

FIG. 6. Rh $3d$ core-level photoemission spectra of an islanded Rh film measured at 150 K and 40° emission angle, upon reversing the magnetization field from M_{up} to M_{down} in chiral geometry. The corresponding LMDAD asymmetry (Ref. 37) is shown in the bottom panel.

bound relatively strongly to the substrate. This bonding, which contrasts with the high mobility required for the formation of the observed Rh islands, may be due to the presence of defects, but we note that no defects were imaged on the clean HOPG by STM prior to the Rh deposition.

The STM topographies confirm that Rh grows onto HOPG at 300 K following the Volmer-Weber mode. This kind of growth has been observed at 300 K also for Ti,[35] Mo,[38] V, Cr, Mn, Fe,[28] and Pd,[39] deposited on graphite. The case of Ru deposited on HOPG represents instead a controversial situation. Pfandzelter, Steierl, and Rau[24] interpreted the attenuation of the carbon Auger signal and the increase of the Ru Auger signal, for Ru deposited at 300 K, as a straight line with change in slope, consistent with the lateral growth of a single layer of Ru/HOPG. They also showed, using spin-polarized secondary-electrons spectroscopy, that this Ru layer has a long-range in-plane magnetic order, providing evidence of magnetism in $4d$ thin films supported on a nonmagnetic substrate.[24] These results have been questioned by Binns *et al.*[28] who, on the basis of photoemission and reflectivity measurements, suggest a Volmer-Weber growth mode at either 300 or 70 K. The attenuation of the C $1s$ photoemission signal at 300 K in the data of Binns *et al.*,[28] where two linear segments with change in slope were identified, is very similar to the behavior of the carbon Auger signal observed by Pfandzelter *et al.*,[24] but their interpretation is different, mainly based on their very clear reflectivity measurements. Binns *et al.*,[28] also failed to observe LMDAD effects on the Ru film grown at 300 K.

Binns *et al.*[28] suggest a 3D island growth of Ru/HOPG also at 70 K where the linear behavior and the change in slope in the attenuation of the C $1s$ photoemission signal are indeed very similar to our XPS data for Rh deposition at 150 K (see Fig. 1). Again, these authors[28] support the XPS data with reflectivity measurements at low temperature, but in this case there are too few experimental points to exclude a layer-by-layer or a Stranski-Krastanov growth mode.

To summarize this section, the above arguments indicate that at 300 K Rh thin films grow on HOPG by forming three-dimensional islands as other $3d$ and $4d$ transition metals do. At 150 K, instead, our XPS and LEED data strongly suggest that Rh grows in a Stranski-Krastanov fashion, where the first layer forms a metastable single pseudomorphic $p(1\times1)$ structure that transforms into an islanded film as the temperature rises.

B. Magnetic properties

We investigated the possible existence of long-range magnetic order in these Rh films by means of LMDAD in core-level photoemission. For a given experimental geometry, photoemission spectra were acquired for two opposite orientations (up and down) of the magnetic field applied parallel to the sample surface, but perpendicular to the scattering plane (chiral geometry). In the presence of in-plane magnetization of the sample, this provides a series of mirror experiments for testing LMDAD effects.[37]

First we looked for magnetic effects in the Rh films deposited or annealed at 300 K, where three-dimensional islands are present. Figure 6 reports the Rh $3d$ core-level photoemission spectra of these films cooled down to 150 K, for the two opposite orientations of the magnetization, showing the absence of a LMDAD signal. A null LMDAD signal has also been observed in presence of a small magnetic field (5

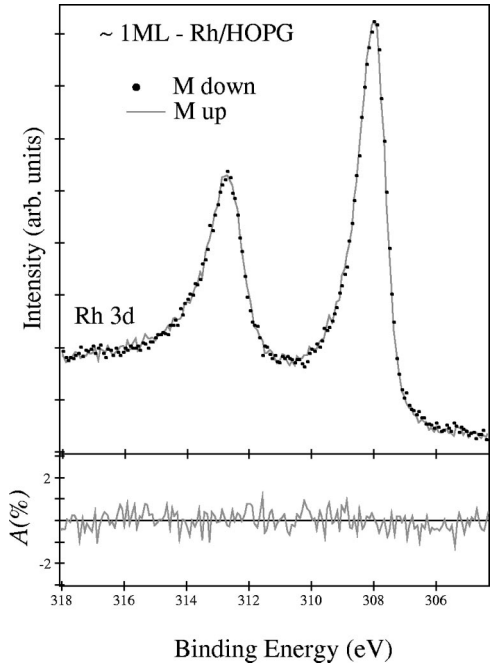

FIG. 7. Rh $3d$ core-level photoemission spectra of 1 ML of Rh deposited at 150 K and measured at 150 K and 40° emission angle, upon reversing the magnetization field from M_{up} to M_{down} in chiral geometry. The corresponding LMDAD asymmetry (Ref. 37) is shown in the bottom panel.

G) applied to the sample. All the available calculations about the possible magnetic configurations of Rh thin films agree in predicting the survival of magnetism only for a single atomic layer. When two or three monolayers are considered, the magnetism is destroyed.[14,20,28] The morphology of the Rh/HOPG films grown or annealed at 300 K is, therefore, unsuitable for retaining long-range ferromagnetic order, which is consistent with the absence of LMDAD in the Rh $3d$ core-level spectra of Fig. 6.

On the other hand, Rh deposited on HOPG kept at 150 K forms a two-dimensional ordered structure (see Sec. III A) that in principle is able to retain a nonzero magnetic moment of the Rh adatoms. Therefore, after a new cleave and cleaning procedure of the HOPG substrate, we repeated the Rh deposition under the same experimental conditions with the HOPG substrate kept at 150 K, stopping it just before the completion of the first layer. Figure 7 shows the Rh $3d$ core levels of this film taken for the two opposite orientations of the magnetization field in chiral geometry. The measurements were performed at 150 K. It is evident that the LMDAD asymmetry is again null, indicating the absence of long-range in-plane magnetic ordering. Even in this case the absence of LMDAD in the photoemission spectra was also verified when a small magnetic field was left on after the magnetization cycle.

There are two possibilities to explain the absence of LMDAD in the photoemission spectra of this Rh film. The first obvious explanation is that the film is nonmagnetic. Although the graphite surface is naively expected to have little influence on the magnetism of the Rh overlayer, recent calculations have disproved this picture.[20,21] The magnetic moments are found to depend strongly on the overlayer/substrate intralayer distance and on the nearest-neighbor distance of the Rh adatoms.[20,21,28] A metal-to-metal distance increased by at least 5% relative to the Rh bulk nearest-neighbor distance (2.69 Å) and an adatom/substrate intralayer spacing larger than 2.5 Å are both crucial conditions for the stabilization of magnetism in single-layer films of Rh/HOPG.[20,21,28]

Our LEED data suggest that the monolayer deposited at 150 K can have a $p(1\times1)$ hexagonal ordered structure with a Rh-Rh distance of 2.46 Å, i.e., the same distance between β sites or the centers of the hexagons as in HOPG. This value corresponds to a contraction of the Rh bulk nearest-neighbor distance of about 9%, which according to the theoretical prediction is unable to preserve the atomic moments. Also, the STM topography of the isolated metallic adatom suggests that Rh atoms are preferentially adsorbed onto β sites, as observed in the case of other $4d$ and $3d$ transition metals.[40] In the above calculations the only stable magnetic configuration of Rh/HOPG is obtained for a $p(2\times2)$ structure of the Rh adatoms, which implies the presence of adatoms on both hollow (centers of the hexagons) and β sites.[20,21,28] It is worth noting that, in these calculations, only the adatoms on a hollow site retain a net magnetic moment, while the magnetic moment of Rh adatoms on β sites is null for any reasonable Rh-C bond distance.[28]

There is a second possible explanation. As shown by recent calculations, in a free-standing Rh monolayer the orientation perpendicular to the surface of the magnetic moments is strongly favored relative to the in-plane orientation.[41] A magnetization perpendicular to the surface breaks the chirality of our experiment and as a consequence LMDAD cannot be observed.

The perpendicular or in-plane orientation of the magnetic moments depends on the magnetocrystalline anisotropy energy, which can be approximated by the band energy difference when the moments are oriented in plane or out of plane. In a free-standing monolayer this quantity is mainly determined by the spin-orbit coupling. In an overlayer system it depends also on the hybridization of the out-of-plane states with the substrate states.[42] For example, in the case of a free-standing monolayer of Co the strong tendency to in-plane orientation of the magnetic moments is found to originate from the spin-orbit coupling between the occupied $d_{xz,yz}$ and unoccupied d_{z^2} and $d_{x^2-y^2}$ states.[42] When adsorbed onto Pd, the $d_{xz,yz}$ states are appreciably pushed up because of the hybridization with the substrate, favoring the perpendicular orientation of the moments.

The above discussion highlights the important role played by the orbital hybridization (Rh-Rh and Rh-C) and by the spin-orbit interaction in the hybrid bands in determining the magnetic properties of Rh/HOPG. The importance of the orbital hybridization is further confirmed by growing a thick Rh layer on HOPG. This system does not present long-range order, but the corresponding Rh $3d_{5/2}$ core level (see Fig. 8) shows a surface component as a clear shoulder on the low-binding-energy side of the photoemission spectrum. By fitting this photoemission spectrum with two components we obtain a surface core-level shift of 415 ± 20 meV at 150 K.

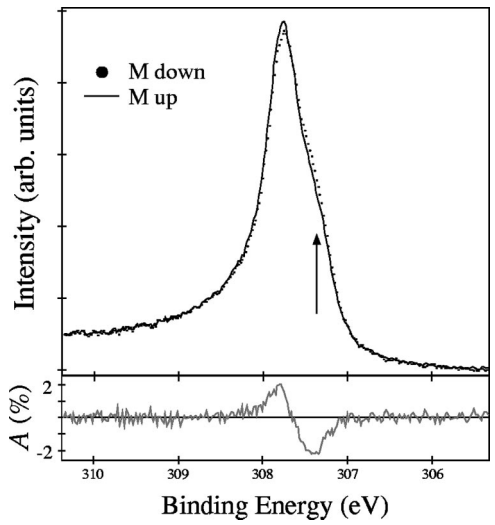

FIG. 8. Rh $3d_{5/2}$ core-level photoemission spectra of a thick Rh layer on HOPG deposited at 300 K and measured at 150 K and 40° emission angle, upon reversing the magnetization field from M_{up} to M_{down} in chiral geometry. The corresponding LMDAD asymmetry is shown in the bottom panel. The arrow indicates the surface component.

This value is comparable to the surface core-level shift observed on Rh(111) at the same temperature (485 ± 20 meV),[43] while for the other low-index surfaces the surface core-level shift is larger.[43–45] Therefore, in the spectra of the Rh thick film, the surface component probably arises from the presence of (111)-terminated Rh islands. Figure 8 reports the Rh $3d_{5/2}$ core level taken for the two opposite orientations of the magnetization field in chiral geometry. In this case, we do observe a LMDAD asymmetry similar to that observed on the Rh(100) surface.[30,45] As in the case of the Rh(100) surface LMDAD effects are observed only when a small magnetic field is left applied to the sample after the magnetization cycle.[45] This result indicates that the Rh atoms at the surface are polarizable, retaining a net magnetic moment. The appearance of magnetic moments, therefore, is not only a phenomenon related to the reduced dimensionality of the system, but strongly depends on the interface structure, the adatom configuration, and nanomorphology.

IV. CONCLUSIONS

We have studied the growth mode and magnetic properties of ultrathin Rh layers deposited on highly oriented pyrolitic graphite using photoemission and scanning tunneling microscopy. At room temperature Rh grows on HOPG by forming 3D islands (Volmer-Weber mode) at every coverage, while it probably forms a commensurate $p(1\times1)$ ordered structure when deposited at 150 K for coverage up to one monolayer. The possible presence of in-plane ferromagnetic ordering in these low-dimensional Rh systems has been checked by means of linear magnetic dichroism in angle-resolved photoemission. For submonolayer or monolayer Rh films on HOPG there is no evidence of in-plane long-range magnetic ordering down to 150 K. In addition, when thick Rh islands were grown we observed the presence of a surface component in the Rh $3d_{5/2}$ core-level photoemission spectra and the appearance of a net magnetic moment in the surface atoms, as in the case of the Rh(100) surface. This suggests that the magnetic properties of Rh atoms are related not only to the reduced dimension of the system, but also to the interaction (orbital hybridization) with the surrounding atoms.

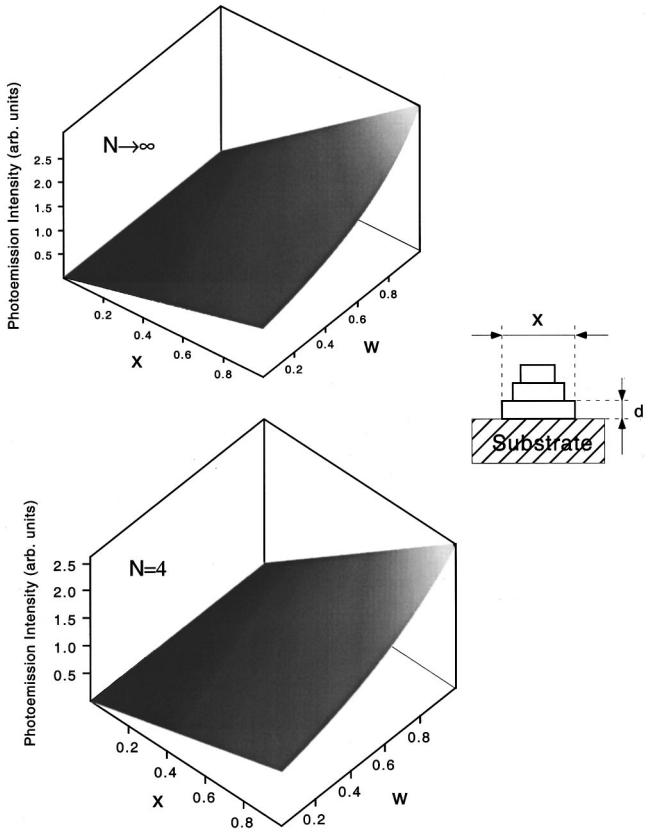

FIG. 9. Photoemission intensity $I(X,W)$ of the overlayer as obtained for a Volmer-Weber growth mode, considering islands formed by $N=4$ layers (bottom) and for $N\rightarrow\infty$ (top) (see Appendix for details). Inset: Schematic representation of the Volmer-Weber model used for the calculations.

APPENDIX

Here we simulate how the signal of the adsorbate should increase in core-level photoemission experiments on noninterdiffusing adsorbate-substrate systems that follow a Volmer-Weber growth. The simple model we use is schematically shown in the inset of Fig. 9. We consider the presence of three-dimensional islands that cover a fraction $X(0 \leqslant X \leqslant 1)$ of the substrate area. We simply assume that all the islands are formed by the same number n of layers (i.e., the islands have the same height). As already shown,[46] this assumption does not compromise a correct understanding of the growth process. Finally, we also assume that the overlap $W(0 \leqslant W \leqslant 1)$ between the different layers in a given island is the same for each layer (i.e., the layer $n+1$ covers a fraction W of the layer n, which also covers a fraction W of the layer $n-1$). This further assumption strongly simplifies the calculations in order to find a recursive formula, but does not

influence the final result, since the same final formula can be obtained by assuming a random overlap between the layers. Under these conditions, it is easy to demonstrate that the photoemission intensity of the growing adsorbate is given by

$$I(X,W) = I_o X \sum_{n=1}^{N} \left[W \exp\left(-\frac{d}{\lambda} \right) \right]^{n-1}$$

$$= I_o X \frac{1 - [W \exp(-d/\lambda)]^{N-1}}{1 - W \exp(-d/\lambda)},$$

where I_o is the overall photoemission signal of one single layer of adsorbate, N is the maximum number of layers present in the islands, d is the thickness of one adsorbate layer, and λ is the electron escape depth. A similar formula has been obtained in another work.[46]

Figure 9 shows $I(X,W)$ for $N \to \infty$ (top panel) and $N=4$ (bottom panel) assuming $d=2$ Å and $\lambda=5$ Å in order to simulate the Rh $3d$ signal in our working conditions. $I(X,W)$ is a concave surface, made by a family of straight lines in X with increasing angular coefficient as W increases. The concavity also depends on N, but in our working conditions for $N>10$ rapidly converges to the limit for $N \to \infty$.

The behavior of the Rh $3d$ signal as a function of the Rh evaporation time reported in Fig. 2 should stay on this surface and, therefore, the observed concave behavior is in perfect agreement with a Volmer-Weber growth. The concave behavior in Fig. 2 is mainly seen in the early stage of growth, while for evaporation times higher than ~330 s the dependence is almost linear. We can understand that at the beginning the growth is dominated by the change in the volume of the islands (change of W) rather than by changes in the number of islands or in the lateral size of the basal plane of the islands (change of X). These latter mechanisms dominate, instead, at higher coverages.

[1] F. J. Himpsel, J. E. Ortega, G. J. Mankey, and R. F. Willis, Adv. Phys. **47**, 511 (1998), and references therein.

[2] R. Allenspach, J. Magn. Magn. Mater. **129**, 160 (1994).

[3] R. Miranda, Surf. Rev. Lett. **4**, 327 (1997).

[4] A. J. Freeman and R. Q. Wu, J. Magn. Magn. Mater. **100**, 497 (1991); R. Q. Wu and A. J. Freeman, Phys. Rev. B **45**, 7222 (1992).

[5] M. N. Baibich, J. M. Broto, A. Fert, A. Dau, F. Petroff, P. Etienne, G. Creuzet, A. Friederich, and J. Chazelas, Phys. Rev. Lett. **61**, 2472 (1988); G. Binash, P. Grunberg, F. Saurenbach, and W. Zinn, Phys. Rev. B **39**, 4828 (1989).

[6] S. N. Khanna and S. Linderoth, Phys. Rev. Lett. **67**, 742 (1991).

[7] B. Dieny, V. S. Speriosu, S. S. P. Parkin, A. B. Gurney, D. R. Wihoit, and D. Mauri, Phys. Rev. B **43**, 1279 (1991); J. M. Daughton, Thin Solid Films **216**, 162 (1992); J. E. Hurst, Jr., and W. J. Kozlovsky, Jpn. J. Appl. Phys., Part 1 **32**, 5301 (1993).

[8] V. L. Moruzzi and P. M. Marcus, Phys. Rev. B **39**, 471 (1989).

[9] S. Blügel, Phys. Rev. Lett. **68**, 851 (1992); Europhys. Lett. **18**, 257 (1992).

[10] R. Q. Wu and J. A. Freeman, Phys. Rev. B **51**, 15 131 (1995).

[11] A. Mokrani, H. Dreyssé, S. Bouarab, and C. Demangeat, J. Magn. Magn. Mater. **113**, 201 (1992).

[12] B. V. Reddy, S. N. Khanna, and B. I. Dunlap, Phys. Rev. Lett. **70**, 3323 (1993); Yang Jinlong, F. Toigo, Wang Kelin, and Zhang Manhong, Phys. Rev. B **50**, 7173 (1994); B. Piveteau, M. C. Desjonquères, A. M. Olés, and D. Spanjaard, Surf. Sci. **352**, 951 (1996); Yang Jinlong, F. Toigo, and Wang Kelin, Surf. Rev. Lett. **3**, 323 (1996).

[13] S. K. Nayak, S. E. Weber, P. Jena, K. Wildberger, R. Zeller, P. H. Dederichs, V. S. Stepanyuk, and W. Hergert, Phys. Rev. B **56**, 8849 (1997).

[14] O. Eriksson, R. C. Albers, and A. M. Boring, Phys. Rev. Lett. **66**, 1350 (1991); M. J. Zhu, D. M. Bylander, and L. Kleinman, Phys. Rev. B **43**, 4007 (1991); L. Kleinman, Int. J. Mod. Phys. B **7**, 482 (1993); P. Rennert, W. Hergert, W. Mück, C. Demangeat, S. Bouarab, and H. Dreyssé, Surf. Sci. **307-309**, 1091 (1994); J. Dorantes-Dávila, A. Mokrani, H. Dreyssé, and C. Demangeat, J. Magn. Magn. Mater. **165**, 268 (1997); W. Hergert, P. Rennert, H. Dreyssé, and C. Demangeat, Surf. Rev. Lett. **2**, 203 (1995).

[15] J. Redinger, S. Blügel, and R. Podloucky, Phys. Rev. B **51**, 13 852 (1995).

[16] B. Ujfalussy, L. Szunyogh, and P. Weinberger, Phys. Rev. B **51**, 12 836 (1995).

[17] C. S. Chang, L. H. Cho, J. I. Lee, S. C. Hong, R. Wu, and A. J. Freeman, J. Magn. Magn. Mater. **177-181**, 1255 (1998).

[18] T. Bryk, D. M. Bylander, and L. Kleinman, Phys. Rev. B **61**, R3780 (2000).

[19] C. Barreteau, R. Guirado-López, D. Spanjaard, M. C. Desjonquères, and A. M. Olés, Phys. Rev. B **61**, 7781 (2000).

[20] P. Krüger, A. Rakotomahevitra, G. Moraitis, J. C. Parlebas, and C. Demangeat, Physica B **237-238**, 278 (1997); P. Krüger, A. Rakotomahevitra, J. C. Parlebas, and C. Demangeat, Phys. Rev. B **57**, 5276 (1998).

[21] L. Chen, R. Wu, N. Kiussis, and J. R. Blanco, J. Appl. Phys. **81**, 4161 (1997).

[22] H. Li, S. C. Wu, D. Tian, Y. S. Li, J. Quinn, and F. Jona, Phys. Rev. B **44**, 1438 (1991).

[23] G. A. Mulhollan, R. L. Fink, and J. L. Erskine, Phys. Rev. B **44**, 2393 (1991); C. Liu and S. D. Bader, *ibid.* **44**, 12 062 (1991).

[24] R. Pfandzelter, G. Steierl, and C. Rau, Phys. Rev. Lett. **74**, 3467 (1995).

[25] A. B. Hayden, T. Valla, and D. P. Woodruff, J. Phys.: Condens. Matter **7**, 9475 (1995).

[26] H. Beckmann and G. Bergmann, Phys. Rev. B **55**, 14 350 (1997).

[27] D. P. Moore, O. Ozturk, F. O. Schumann, S. A. Morton, and G. D. Waddill, Surf. Sci. **449**, 31 (2000).

[28] C. Binns, S. H. Baker, C. Demangeat, and J. C. Parlebas, Surf. Sci. Rep. **34**, 105 (1999), and references therein.

[29] J.-H. Cho and M. Scheffler, Phys. Rev. Lett. **78**, 1299 (1997).

[30] A. Goldoni, A. Baraldi, G. Comelli, S. Lizzit, and G. Paolucci, Phys. Rev. Lett. **82**, 3156 (1999).

[31] A. J. Cox, J. G. Louderback, and L. Bloomfield, Phys. Rev. Lett. **71**, 923 (1993); A. J. Cox *et al.*, Phys. Rev. B **49**, 12 295 (1994).

[32] P. Krüger, M. Taguchi, J. C. Parlebas, and A. Kotani, Phys. Rev. B **55**, 16 466 (1997).
[33] D. M. Duffy and J. A. Blackman, Phys. Rev. B **58**, 7443 (1998).
[34] P. Krüger, J. C. Parlebas, and A. Kotani, Phys. Rev. B **59**, 15 093 (1999).
[35] Q. Ma and R. A. Rosenberg, Phys. Rev. B **60**, 2827 (1999).
[36] A. Abrami *et al.*, Rev. Sci. Instrum. **66**, 1618 (1995).
[37] Ch. Roth, F. U. Hillebrecht, H. B. Rose, and E. Kisker, Phys. Rev. Lett. **70**, 3479 (1993); G. Rossi, F. Sirotti, N. A. Cherepkov, F. Combet Farnoux, and G. Panaccione, Solid State Commun. **90**, 557 (1994); G. Rossi, F. Sirotti, and G. Panaccione, in *Core Level Spectroscopies for Magnetic Phenomena*, Vol. 345 of *NATO Advanced Study Institute, Series B: Physics*, edited by P. S. Bagus, G. Pacchioni, and F. Parmigiani (Plenum Press, NY, 1995), p. 181.
[38] H. Xu, H. Permana, Y. Lu, and K. Y. S. Ng, Surf. Sci. **325**, 285 (1995).
[39] H. Y. Nie, T. Shimizu, and H. Tokumoto, J. Vac. Sci. Technol. B **12**, 1843 (1994); A. Bifone, L. Casalis, and R. Riva, Phys. Rev. B **51**, 11 043 (1995).
[40] E. Ganz, K. Sattler, and J. Clarke, Surf. Sci. **219**, 33 (1989).
[41] R. Gomez-Abal and A. M. Llois, Phys. Rev. B **60**, 12 841 (1999).
[42] A. J. Freeman, Ruquian Wu, Miyoung Kim, and V. I. Gavrilenko, J. Magn. Magn. Mater. **203**, 1 (1999), and references therein.
[43] M. V. Ganduglia-Pirovano, M. Scheffler, A. Baraldi, S. Lizzit, G. Comelli, G. Paolucci, and R. Rosei (unpublished).
[44] A. Baraldi, G. Comelli, S. Lizzit, M. Kiskinova, G. Paolucci, and R. Rosei (unpublished).
[45] A. Goldoni, A. Baraldi, G. Comelli, S. Lizzit, and G. Paolucci, Surf. Sci. **454-456**, 925 (2000).
[46] S. Ossicini, R. Memeo, and F. Ciccacci, J. Vac. Sci. Technol. A **3**, 387 (1985).